JASA

ARTICLE

Restricting angles of incidence to improve super resolution in time reversal focusing that uses metamaterial properties of a resonator array

Andrew Basham,[1] Brian E. Anderson,[1,a)] and Adam D. Kingsley[1,2]

[1]*Acoustics Research Group, Department of Physics and Astronomy, Brigham Young University, Provo, Utah 84602, USA*

[2]*RDA Inc., Warrenton, Virginia 20187, USA*

ABSTRACT:

Focusing waves with a spatial extent smaller than a half wavelength (i.e., super resolution or sub diffraction limit) is possible using resonators placed in the near field of time reversal (TR) focusing. While a two-dimensional (2D) Helmholtz resonator array in a three-dimensional reverberant environment has limited ability to produce a high-resolution spatial focus in the TR focusing of audible sound, it is shown that acoustic waves propagating out-of-plane with the resonator array are not as strongly affected by the smaller effective wavelength induced by the resonator array, partially negating the effect of the resonators. A physical 2D waveguide is shown to limit the out-of-plane propagation, leading to improved resolution. It is also shown that post processing using an orthogonal particle velocity decomposition of a spatial scan of the focusing can filter out-of-plane particle motion in the near field of the array, which bypasses the effect of the unwanted third spatial dimension of propagation. The spatial resolution in a reverberant environment is shown to improve in the presence of a 2D Helmholtz resonator array and then further improve by adding a 2D waveguide. The resolution among the resonator array is better still without using a waveguide and instead using the partial-pressure reconstruction. © 2024 Acoustical Society of America.
https://doi.org/10.1121/10.0025987

I. INTRODUCTION

Acoustic imaging is the use of acoustic waves to characterize a sound source, such as the ultrasound methods commonly used in medical imaging applications.[1,2] There is an interest in many applications to achieve the highest resolution possible. Acoustic imaging is limited, however, in its ability to resolve point sources from each other in the far field due to the diffraction limit. The diffraction limit has been defined in various ways, but all aim to define the physical limit of resolution achievable by a propagating wave.[3] Here, we use the common definition of the half wavelength ($\lambda/2$), of the full width at half-maximum (FWHM) of the spatial extent of the focusing (or $\lambda/4$ for intensities).[3] For a focus comprised of a finite bandwidth, the strictest definition is to assume λ is the wavelength of the highest frequency of the bandwidth, which we adopt here.

Focusing and imaging are directly related to one another, which makes improvements in focusing techniques an important part of improving imaging applications as well.[1] The method of acoustic focusing used here is time reversal (TR). TR is a signal processing technique that has been employed to focus waves in the electromagnetic, ultrasonic, and aeroacoustic domains.[4–6] Reciprocal TR is performed in a two-step process between emitting transducers and a receiver placed at the desired focal location.[5] The forward step is simply obtaining an impulse response between each emitting transducer and the receiver; the backwards step has each emitting transducer simultaneously play back a time-reversed version of its corresponding impulse response obtained in the forward step. These emissions time align reflections and direct sound propagation such that they constructively interfere at the receiver position to approximately reconstruct the original impulse. In this paper, a chirp signal is emitted during the forward step and the impulse response is obtained through cross correlation of the chirp signal and the response to the chirp signal.[7,8]

The first use of TR was for underwater communication applications.[9] TR has subsequently been used in a variety of communication applications, including underwater,[10–13] airborne,[14–16] and elastic[17] communications. It is also been used for high amplitude focusing[18] for medical applications,[19–21] nondestructive evaluation,[6,22] and in generating loud sounds in air.[23–26] Finally, TR has been used for source reconstruction and imaging, including application to earthquakes,[27–30] touchpad taps,[31,32] and gunshot localization.[33,34] A visual demonstration of knocking over targeted LEGO minifigures using TR has been developed.[35,36]

Contrary to what is typical with other focusing methods like beamforming, TR excels in reverberant environments and with complex geometries. Not only does it not suffer from such complexity, it actually exploits large amounts of

a)Email: bea@byu.edu

reverberation to deliver even more coherent energy to the focus by turning reflected sound into virtual sources, thus creating a wider angular aperture. However, even under ideal circumstances the best focus resolution possible for a TR focus is defined by the diffraction limit, $\lambda/2$.[37]

Recent explorations have achieved subwavelength focusing, or super resolution, by the use of an array of resonators in the near field of the focus (though other techniques besides using resonators have been used as well, see reviews in Refs. [38] and [39]). Lerosey et al.[40] set up an arrangement of resonating wire antennae and demonstrated $\lambda/30$ resolution (the antenna spacing). Lemoult et al.[41,42] then extended this idea to focusing sound among an array of Helmholtz resonators comprised of common soda cans. The emitting transducers were placed equidistant to the intended location of the focus over one of the soda cans (the transducers were in the same plane as the can array) and emitted sound in short pulses, time-aligned using TR. It was shown that this focusing excites subwavelength phononic eigenmodes in the resonator lattice, enabling the subwavelength focusing. This method resulted in a focus resolution of $\lambda/8$, which was improved to $\lambda/25$ using iterative TR methods. With a similar experimental setup, Maznev et al.[43] established that as the frequency of the time aligned waves approaches that of the resonance frequency of an individual Helmholtz resonator (420 Hz), the spatial resolution increases. They showed that the resonator array acts as an effective medium that decreases the effective wavelength of waves below the Helmholtz resonance. Their work also demonstrated that TR was not necessary for subwavelength focusing in this configuration. Kingsley et al.[39] explored the trade-off in resolution of TR focusing among an array of resonators versus the amplitude of that focusing, the impact of the resonator shape on these factors, and the dual-nature aspects of the array of resonators acting together as an effective medium and the discrete impacts of each resonator on the focusing using equivalent circuit modeling. Kingsley and Anderson[44] then verified this circuit model with finite-element, full-wave modeling, and the ability of a single resonator to slow down passing waves was illustrated. Finally, Kingsley et al.[45] experimentally demonstrated that super resolution focusing with a resonator array is possible in a reverberant environment and showed that it could be used to image multipole sources.

Aside from the work reviewed by Kingsley et al., all previous work with the soda can arrangement was restricted to direct sound arrivals from in-plane sources. Lerosey et al. utilized a reverberant electromagnetic environment, but resonator array experiments have not been performed much in acoustic reverberant environments, other than Kingsley's work. Kingsley et al.[45] used sources that were not in plane and utilized significant reverberation in their TR experiments (the same as we will do here). The degree to which super resolution depends on the angle of incidence of the focused waves has not yet been explored. Super resolution focusing is achievable with only in-plane waves as demonstrated by Lemoult et al. and Maznev et al., who only utilized waves incident upon the cans in the in plane direction. The inclusion of out-of-plane waves apparently does not prevent super resolution focusing as demonstrated by Lerosey et al. and Kingsley et al. but it has yet to be shown whether the inclusion of out-of-plane waves improve or hamper the resolution, and if it hampers the resolution, if there are ways to eliminate the out-of-plane waves. Nonplanar incident waves contribute effectively longer wavelengths (their projections in plane are called "trace wavelengths") to the in-plane wave field and thus should inhibit the potential for super resolution focusing.

The purpose of this work is to demonstrate that the elimination of out-of-plane waves improves super resolution focusing when focusing among an array of resonators and we propose a couple of ways to achieve this. We use a soda can array in a reverberation chamber and eliminate out-of-plane waves by imposing a physical waveguide, or alternatively, by using wave field decomposition. We demonstrate experimentally that super resolution focusing improves when the soda can array is encased in a two-dimensional (2D) waveguide, since the waveguide only allows propagation of in-plane waves among the resonator array. Next, using calculated particle velocity components of experimentally obtained data in post processing, a partial pressure field that excludes the out-of-plane component of particle motion further improves the spatial resolution of the focus. Each technique shows that the in-plane components of incident waves are preferred for maximizing the resolution of the focus. A characterization of the spatial extent of the focusing outward from the soda can array (out-of-plane direction) is also provided.

A metamaterial resonator array can be considered a phononic crystal,[40,42,46] and as such, many applications have been proposed. Here, we mention a few. Wave propagation among the phononic crystal can be controlled to change the direction of the waves on a sub-wavelength scale.[46] It has also been shown that if a resonator is removed from the array, this defect in the crystal can be localized.[42] The final application we will mention here is that metamaterial resonator arrays have been proposed as devices that can be used, along with TR, to locate damage in a medium because the damage is the source of nonlinear frequency content.[47,48] The present research discussed illustrates the importance of using waves that propagate in the plane of the metamaterial and avoiding using waves that propagate out-of-plane in order to maximize the potential for these proposed applications.

II. EXPERIMENTAL SETUP

All experiments are performed in the large reverberation chamber at Brigham Young University having dimensions of $4.96 \times 5.89 \times 6.98$ m. Its overall reverberation time is 6.85 s and its Schroeder frequency is 355 Hz, above which the chamber is assumed to contain a diffuse field. In these experiments, eight HR824mk2 Mackie loudspeakers (Mackie, Seattle, WA) are placed randomly around the

Basham et al.

perimeter of the chamber. An example of their arrangement is shown in Fig. 1(a). The loudspeakers are intentionally pointed away from the focal location to maximize the impact of the reverberation in the reversed impulse responses.[8] Figure 1(a) also shows a mechanical scanning gantry with two dimensions each controlled by an Applied Motion Products STAC 6i (AMP, Morgan Hill, CA) controller and an Applied Motion Products HT23-550D stepper motor. The translation stage of the gantry has dimensions of 2×2 m and holds a GRAS 46AQ (GRAS, Holte, Denmark) 1.27 cm (1/2 in.) random-incidence microphone used to iteratively probe the spatial extent of a wave field of interest in two dimensions. The microphone is powered by a GRAS 12AX CCP power module.

The TR experiments are performed using a computer with three Spectrum Instrumentation (Grosshansdorf, Germany) PCI cards, two M2i.6022 generator cards (containing one channel for each of the eight loudspeakers) and one M2i.4931 acquisition card for the microphone receiver. All channels on the generator and acquisition cards are time synchronized using a Spectrum Star-Hub module. ESTR,[49] a LabVIEW-based software, is used as a user interface to operate the cards, the acoustic equipment, the mechanical scanning gantry, and efficiently perform TR experiments.

An example of the implementation of a TR experiment is Illustrated in Fig. 2. With the receiver placed in the user-selected focus position, a two-second duration, linear chirp signal (360–420 Hz) with some buffering zeros [see Fig. 2(a)] is played from each loudspeaker individually and the response to each chirp are recorded [Fig. 2(b)]. Figure 2(c) shows an example of a time-reversed impulse response generated from a cross correlation of the signals in (a) and (b). Eight reversed impulse responses are computed from each of the eight chirp responses. All eight reversed impulse responses are broadcast simultaneously from the respective loudspeakers to create a TR focus, measured by the microphone receiver at the focus position. An example of a focus signal is shown in Fig. 2(d). A spatial characterization of the focus is simply obtained by repeating the measured focus while measuring the field at different locations with the microphone, whose recordings are time synchronized.

Just as previous experiments have used soda cans as Helmholtz resonators (420 Hz), this experiment follows suit, with 37 cans tightly arranged in a hexagonal array [pictured in Fig. 1(b)]. Adjacent can openings are thus spaced 6.60 cm apart (0.081 λ apart at 420 Hz) for the closest spacing of openings in the array. The cans are magnetically mounted on a board with its plane perpendicular to the ground to accommodate the vertical orientation of the scanning gantry. The resonator array is elevated more than a meter above the floor to minimize unwanted amplitude increases from approaching a reflecting surface[50] and remain within the diffuse zone of the chamber.[51] Each spatial scan measured here consists of a 60×60 cm scan area with a grid spacing of 1 cm, which is large enough to measure the field covering and parallel to the entire resonator array; the 1 cm spacing was chosen since it is smaller than the opening of a can, thus ensuring we would always have a scan position near to each can opening. In each scan, the focus is directed over the mouth of the center can in the array and the head of the microphone is 1 cm away from the openings of the soda cans.

Although a maximal bandwidth is ideal, the bandwidth of 360–420 Hz used in this experiment was chosen because of the Schroeder frequency of the reverberation chamber and to stay below the resonance frequency of the individual resonators in the soda can array, which provide the lower and upper limit of bandwidth respectively. Below the Schroeder frequency (355 Hz), distortion from room mode excitation may occur, and above the resonance frequency of the soda cans (420 Hz), the waves are significantly attenuated and no longer experience the shorter effective wavelength that the resonator array is intended to produce.[44]

III. RESULTS

A. Focusing with and without a resonator array

As a baseline measurement, the first experiment is a characterization of the spatial extent of the focusing when
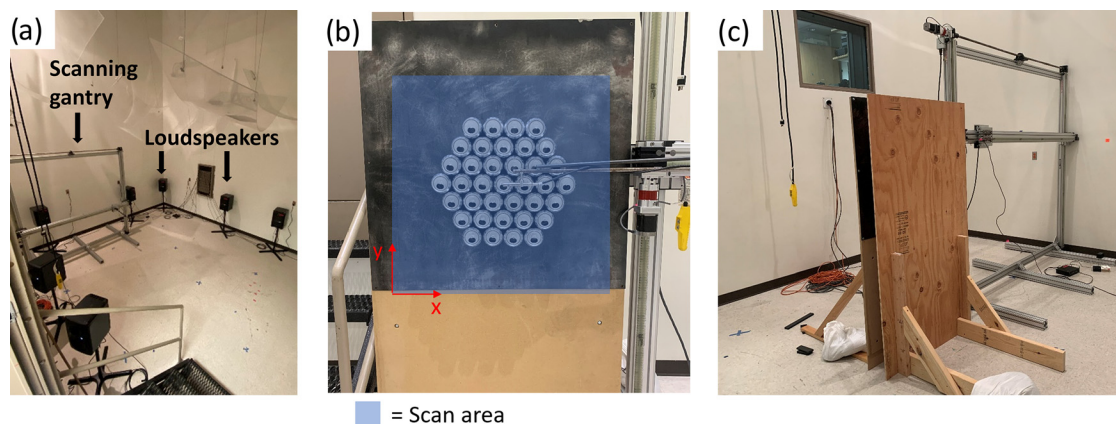

= Scan area

FIG. 1. (Color online) (a) Photograph of the reverberation chamber with seven of the loudspeakers visible, along with the microphone scanning gantry. (b) Photograph of the microphone arm from the scanning apparatus (visible on the right) with the soda can array, with the microphone placed at the focus position near the opening of the center can. The blue area depicts the area over which the scan of the focus is performed. The Cartesian reference frame used to discuss the apparatus and results is defined with red arrows and text. (c) Photograph of the physical 2D waveguide used to restrict out-of-plane incidence angles.

J. Acoust. Soc. Am. **155** (5), May 2024
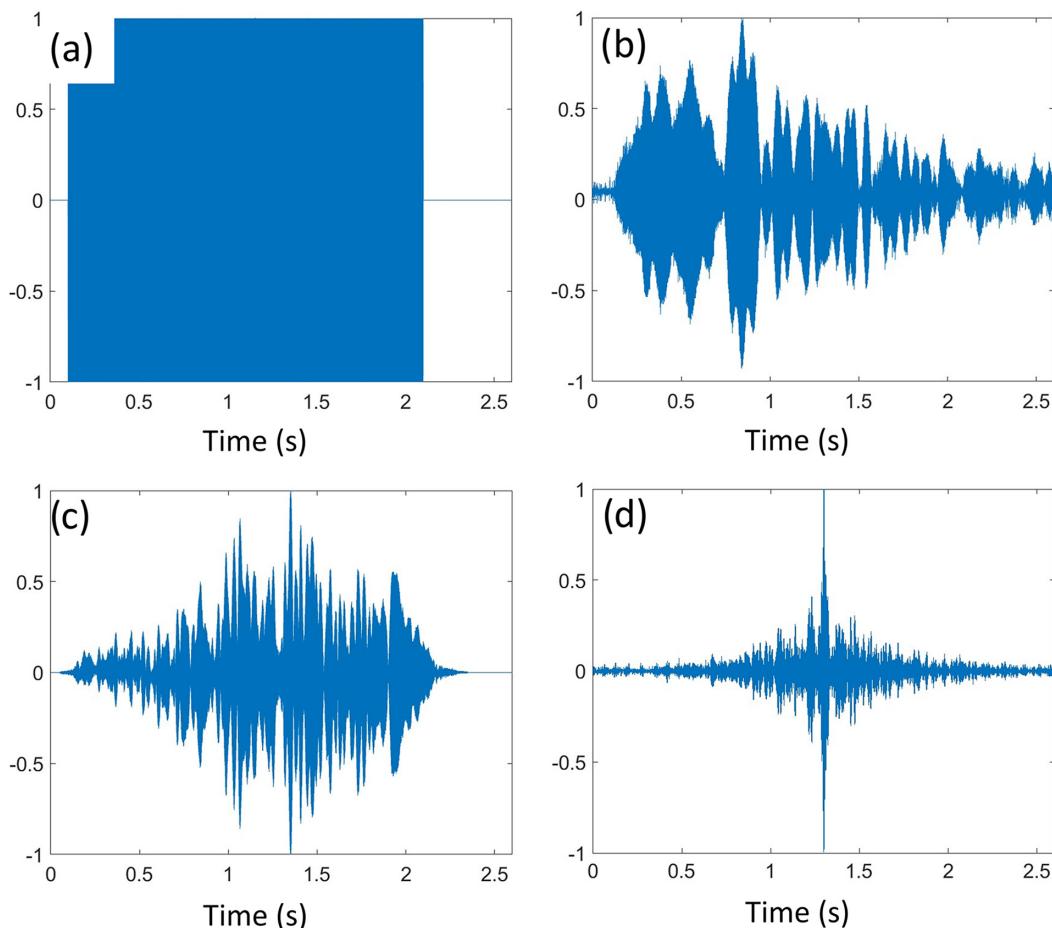
Basham *et al.*   3235

FIG. 2. (Color online) Example signals for a TR experiment with normalized amplitudes. (a) The 360–420 Hz chirp signal played separately by each loudspeaker. (b) Example of a chirp response, recorded at the microphone placed at the focus location, unique for each loudspeaker. (c) A time-reversed impulse response [cross correlation of the signals in (a) and (b)]. (d) A focus recorded at the focus location, generated as all loudspeakers play their corresponding signals from (c).

no array of cans is present at the focus position. The best possible resolution in this case would be that of the diffraction limit. A cross section of the instantaneous, squared sound pressure amplitude versus space is displayed in Fig. 3(a) at the time of maximal focusing (focal time). A squared sine wave of the highest frequency in the bandwidth, 420 Hz ($\lambda = 81.7$ cm), is also plotted to illustrate the tightest possible resolution with this bandwidth. In this case, the width of the no-can TR focusing is wider than that of the highest frequency, which is understandable since the focusing contains a finite bandwidth of frequencies, all of which have larger wavelengths than the highest frequency in the band. Additionally, the point spread function of the focused waves' aperture can often cause the TR focusing to be wider than the diffraction limit. The FWHM of the intensity of the highest frequency is 20.4 cm $= \lambda/4\,(0.25\lambda)$. In this case, the FWHM of the focusing is 38.1 cm, so 0.47λ (187% of the diffraction limit).

Next, a characterization of the spatial extent of a TR focus over the soda can array is given. Figure 3(b) displays x and y cross-sections of the instantaneous squared pressure of the focus at focal time in comparison with the diffraction limit. The narrower FWHM of the two cross-sections is

10.0 cm, which is $10.0/81.7 = 0.122\lambda$ (approximately $\lambda/8$). This is the same resolution as reported in similar experiments that have been done in anechoic environments.[42] However, in those experiments, the median frequency of the bandwidth (400 Hz) was used to define the diffraction limit, instead of using their highest frequency, 600 Hz. If the highest frequency were used, then it would be 0.19λ. Thus, our results are 36% narrower than their reported resolution (higher resolution); this can be attributed to the difference between an anechoic measurement (utilizing only the direct sound that arrives in plane) versus a reverberant measurement (utilizing a lot of reverberation in the impulse response, including waves arriving from all angles of incidence).

B. Physical 2D waveguide

Kingsley *et al.* showed that phase lagging can occur for waves passing over resonators below the resonance frequency of a single resonator in a one-dimensional waveguide and hypothesized that these phase lags can effectively lead to a decrease in the effective phase speed of the resonator array allowing the sub-diffraction limited focusing.[44]
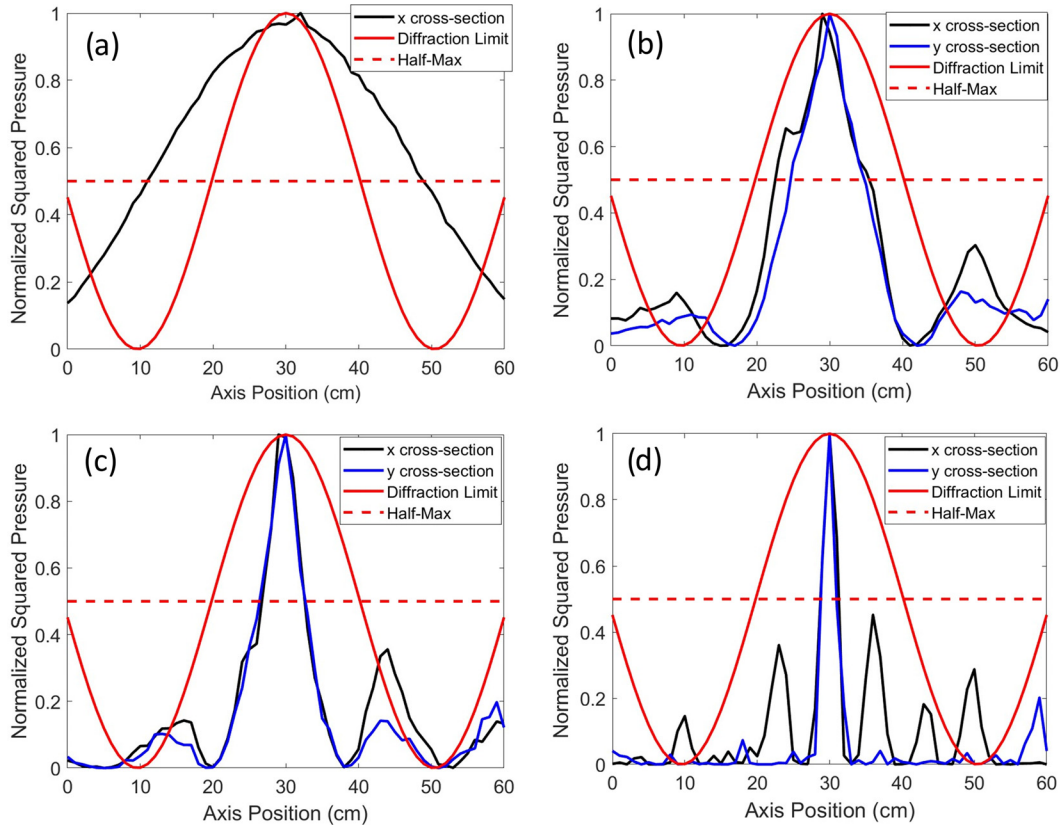
FIG. 3. (Color online) A comparison of four different cases of TR focusing, showing cross-sections of the spatial extent of the instantaneous squared pressure at focal time with amplitude normalized for comparison. (a) A TR focus in the reverb chamber with no cans present. (b) A TR focus over the soda can array. (c) A TR focus with the 2D waveguide and the soda can array. (d) A post-processing partial pressure reconstruction of a focus with the soda can array and no waveguide.

Noting that such a setup can be extended to the 2D waveguide, a parallel reflecting barrier wall with identical dimensions to the board holding the cans is placed about 6 cm away from the openings of the soda cans to create a waveguide [see Fig. 1(c)], allowing space for the scanning microphone to fit between the soda cans and the barrier. The resulting distance between the boards is $L = 18$ cm. The additional board prevents waves from arriving perpendicular to the plane of the array and this waveguide also blocks unwanted cross-mode propagation in the waveguide. The well-known waveguide cutoff frequency f_{01} defines the frequency, below which, only plane waves can propagate within the waveguide (or the lowest frequency limit at which the first order cross-mode propagates in the waveguide)[52] and is given by

$$f_{01} = \frac{c}{2L}, \tag{1}$$

where $c = 343$ m/s defines wave speed and waveguide spacing L is smaller than the other dimensions of the waveguide. For this waveguide, $f_{01} = 953$ Hz, much greater than 420 Hz, the highest frequency in the bandwidth. The soda cans are placed in the center of the waveguide to avoid the evanescent propagation of cross-modes into the waveguide, which typically only propagate into the waveguide a distance corresponding to the 18 cm waveguide dimension.

Acoustic waves passing over the soda cans within the waveguide are thus assumed to be plane waves and propagate only in plane.

When the waveguide is added to the setup, the spatial extent of the TR focusing over the resonator array notably reduces down to $0.070\,\lambda$, a 43% improvement compared to the focusing among the resonator array without the waveguide present. This corresponds to approximately $\lambda/14$.

C. Wave field decomposition

Due to the practical limiting nature of using a 2D waveguide in three-dimensional applications, we explore a method to replace its function while still improving the spatial focus resolution. The goal of this method is to mathematically impose a condition to remove the out-of-plane (z-directional) component in the wave field to approximate the acoustic behavior of the 2D waveguide. When the spatial extent of the TR focus is measured in a 2D array coplanar with the resonator array (in the x- and y-dimensions), a 2D pressure gradient may be easily computed, but there is little direct information about the z-direction component (out-of-plane). However, a post processing technique using a combination of well-known linearized equations in acoustics allows us to disregard the z component of particle motion.

As shown by Ref. 53, Euler's equation,

J. Acoust. Soc. Am. **155** (5), May 2024

Basham *et al.*   3237

$$\vec{u} = -\frac{1}{\rho_0} \int_0^t \vec{\nabla} p \, dt, \qquad (2)$$

can be used to determine the components of particle velocity ($\vec{u}$) coplanar with the measured array, where ρ_0 is equilibrium fluid density, $\vec{\nabla} p$ is the gradient of the pressure, and dt is the time step of the pressure measurements. At this point, it does not matter that the z-component of particle velocity is unknown, because the desired $u_z = 0$ condition can be artificially imposed, which eliminates out-of-plane motion similar to how the physical 2D waveguide does. Although the motion of the air in the resonators will be mostly z-directional, it is the information carried in-plane with the resonator array, modified by the superoscillatory effects (subwavelength phononic eigenmodes) of the resonator array, that contributes to the super resolution [2,6].

Next, the equation of continuity,

$$\frac{d\vec{\rho}}{dt} = -\rho_0 \vec{\nabla} \cdot \vec{u}, \qquad (3)$$

and the equation of state,

$$p = \rho c^2, \qquad (4)$$

can be combined into an Eq. (5), which will allow us to use the previously obtained velocity components in a reconstruction of a partial pressure field (having only x and y components)[54] with the newly imposed condition of invariance in the z-direction,

$$\frac{1}{c^2} \frac{dp}{dt} = -\rho_0 \left[\frac{du_x}{dx} + \frac{du_y}{dy} + \frac{du_z}{dz} \right],$$
$$p = -\rho_0 c^2 \int_0^t \left[\frac{du_x}{dx} + \frac{du_y}{dy} + \frac{du_z}{dz} \right] dt, \qquad (5)$$

where it is assumed that $du_z/dz = 0$. This reconstructed, partial pressure field thus only preserves in-plane waves and thus eliminates the out-of-plane incident waves as the physical waveguide does. In summary, Eq. (2) is used to calculate in-plane velocities from the spatial scan of the measured pressure (in a plane-parallel to the can array), Eq. (5) is then used to construct a partial pressure field due to only in-plane velocities (implicitly setting the out-of-plane velocity equal to zero), and finally broadcasting the reversed partial pressure signals from the loudspeakers to focus waves in the in-plane directions (similar in purpose to the physical waveguide).

Applied to experimental data in post processing, as shown in Fig. 3(d), this method yields a reconstructed focus with a FWHM of 2.1 cm, which constitutes 0.026λ (approximately $\lambda/39$), a 79% improvement in spatial resolution over the original data measured over the soda can array, and a 63% improvement over using a physical waveguide, allowing the TR focus to clearly distinguish an individual resonator in the array.

We conclude this section by discussing the frequency content in the focal signals obtained at the central focal location. Recall that the highest frequency in the bandwidth, 420 Hz, is the one used to define the diffraction limit rather than using the frequency in the middle of the band or a central frequency. If a central frequency of the bandwidth is used to define the diffraction limit then one way to beat the diffraction limit is to simply shift the frequency content to have the majority of its energy be above that central frequency. Figure 4 displays the spectrum of the focal signal obtained when no cans (nor waveguide nor decomposition) are used, when just the array of cans is present (no waveguide or decomposition), when the waveguide is present, and when wave-field decomposition is used. It is interesting to note that, if anything, the spectral content shifts to lower frequencies when the cans are present for the focusing, regardless of whether the waveguide is used or decomposition is used. Thus it is clear that the super resolution observed is not the result of shifting the spectral content to higher frequencies. While not shown, there is no spectral content above the background noise outside of the frequency band shown in Fig. 4 for any of the spectra.

D. z-Extent of focusing

Finally, an experimental characterization of the out-of-plane extent of a focus over the soda can array (with no waveguide or post-processing performed) is given. Previously, Maznev et al.[43] briefly modeled the out-of-plane extent at two different frequencies in a finite element model. A 2D spatial scan in the (y, z) plane is aligned with a row of cans in the array, the TR focus is directed at the mouth of the center can (at $y = 30$ and $z = 0$), and the pressure wave field is measured (a plane perpendicular to the resonator array). Figure 5 (top) shows a plot of the instantaneous squared pressure map at the focus time and a visible evanescent decay of the focus moving outward from the resonator array is apparent in the z-direction, with individual resonators indistinguishable more than about 3 cm from the openings of the soda cans. Figure 5 (bottom) is a profile of the squared pressure along the z-axis directly out from the focus.
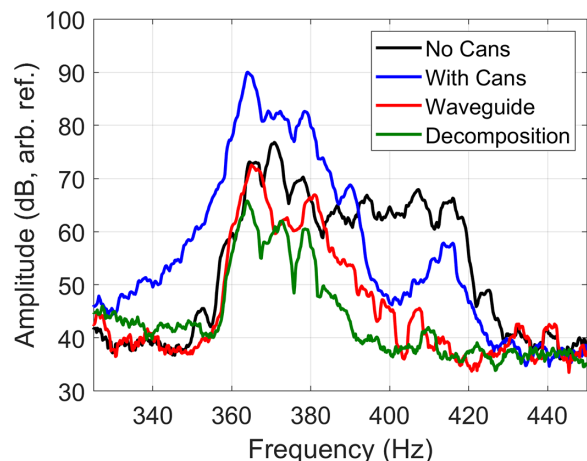

FIG. 4. (Color online) Comparison of frequency spectra of the TR focal signals with no cans, with cans present, when using the waveguide, and when using wave-field decomposition. The frequency band used is 360–420 Hz.
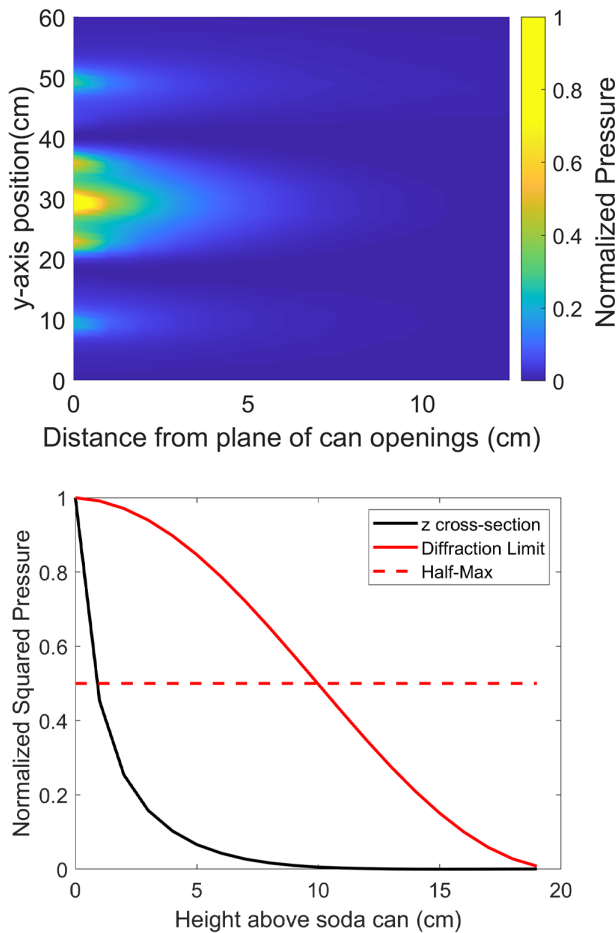
FIG. 5. (Color online) (Top) An out-of-plane view in the (y, z) plane of the spatial distribution of the instantaneous squared pressure map at the focus time of a TR focus over the soda can array. (Bottom) A cross section view of the z-extent of the focus compared against the diffraction limit.

Comparing the z extent of the focus against the diffraction limit shows a focal width that is 2.0 cm, or $0.024\,\lambda$ (approximately $\lambda/41$).

IV. CONCLUSION

TR has been used to focus waves among an array of resonators. The meta material resonator array (or phononic crystal) allows waves to be focused to a spatial extent that is smaller than the diffraction limit (smaller than half of a wavelength at the full width half maximum) for the wavelengths that would exist in free space. It has been shown here that eliminating the out-of-plane incident waves provides tighter spatial focusing than when those waves are included, further beating the diffraction limit. A 2D physical waveguide was used to eliminate the out-of-plane incident waves and this resulted in improved focusing. Additionally, one may avoid using a physical waveguide by scanning the in-plane wave field in the plane of the resonator array and constructing a partial pressure field that does not contain the out-of-plane wave components. This post processing technique also provides improved focusing (tighter spatial

extent) due to the elimination of the out-of-plane incident waves.

Performing the TR focusing among a resonator array metamaterial in a reverberant environment resulted in $0.122\,\lambda$ (approximately $\lambda/8$), 36% narrower than the $0.19\,\lambda$ obtained in previous results that utilized only the direct sound.[42] Recall that we use the highest frequency in the bandwidth to define the diffraction limit. The use of a 2D waveguide parallel plane to the soda can array plane resulted in a higher resolution focusing than without the waveguide of $0.070\,\lambda$ (approximately $\lambda/14$), a 43% improvement compared to the focusing among the resonator array without the waveguide present. The post processing technique that decomposes the particle velocities and reconstructs a partial pressure field results in a resolution of 0.026λ (approximately $\lambda/39$), a 79% improvement in spatial resolution over the result without the waveguide or the decomposition technique, and a 63% improvement over using a physical waveguide. Finally, it is shown that the spatial extent of the focus in the out-of-plane direction relative to the soda can array plane has an exceptional resolution (without a waveguide or post-processing of the data) of $0.024\,\lambda$ (approximately $\lambda/41$). This is due to the apparent exponential decay of amplitude with distance as you move away from the mouth of the soda can.

As Maznev *et al.*[37] asserted, we also suggest that the physics of the diffraction limit is not technically violated in these experiments. Relative to TR focusing in free space (away from the resonator array) we have achieved much better focusing, but the boundary conditions have been greatly changed due to the soda can array, so the effective wavelength is much smaller due to these boundary conditions in the metamaterial. However, the soda can array can be thought of as an effective medium modifying the phase and/or wavelength of the incident waves of the focus, making it possible to achieve a superior focus resolution than what would otherwise be possible in free space. This can be useful across many focusing and imaging/source reconstruction applications.

AUTHOR DECLARATIONS
Conflict of Interest

The authors have no conflicts of interest to disclose.

DATA AVAILABILITY

The data that support the findings of this study are available from the corresponding author upon reasonable request.

J. Acoust. Soc. Am. **155** (5), May 2024

Basham *et al.*   3239

[1] P. N. Keating, T. Sawatari, and G. Zilinskas, "Signal processing in acoustic imaging," Proc. IEEE **67**(4), 496–510 (1979).

[2] M. Kompis, H. Pasterkamp, and G. R. Wodicka, "Acoustic imaging of the human chest," Chest **120**(4), 1309–1321 (2001).

[3] M. Born, E. Wolf, A. B. Bhatia, P. C. Clemmow, D. Gabor, A. R. Stokes, P. A. Wayman, W. L. Wilcock, and P. L. Knight, *Principles of Optics* (Cambridge University Press, Cambridge, UK, 2020).

[4] M. Fink, "Time reversed acoustics," Phys. Today **50**(3), 34–40 (1997).

[5] B. E. Anderson, M. Griffa, C. Larmat, T. J. Ulrich, and P. A. Johnson, "Time reversal," Acoust. Today **4**(1), 5–16 (2008).

[6] B. E. Anderson, M. C. Remillieux, P.-Y. Le Bas, and T. J. Ulrich, "Time reversal techniques," in *Nonlinear Acoustic Techniques for Nondestructive Evaluation*, 1st ed., edited by T. Kundu (Springer and Acoustical Society of America, New York, 2018), pp. 547–581.

[7] B. Van Damme, K. Van Den Abeele, Y. Li, and O. Bou Matar, "Time reversed acoustics techniques for elastic imaging in reverberant and non-reverberant media: An experimental study of the chaotic cavity transducer concept," J. Appl. Phys. **109**(10), 104910 (2011).

[8] B. E. Anderson, M. Clemens, and M. L. Willardson, "The effect of transducer directivity on time reversal focusing," J. Acoust. Soc. Am. **142**(1), EL95–EL101 (2017).

[9] A. Parvulescu and C. S. Clay, "Reproducibility of signal transmissions in the ocean," Radio Electron. Eng. UK **29**(4), 223–228 (1965).

[10] D. R. Jackson and D. R. Dowling, "Phase conjugation in underwater acoustics," J. Acoust. Soc. Am. **89**, 171–181 (1991).

[11] G. F. Edelmann, H. C. Song, S. Kim, W. S. Hodgkiss, W. A. Kuperman, and T. Akal, "Underwater acoustic communications using time reversal," IEEE J. Oceanic Eng. **30**(4), 852–864 (2005).

[12] H. C. Song, "An overview of underwater time-reversal communication," IEEE J. Oceanic Eng. **41**, 644–655 (2016).

[13] H. C. Song and W. A. Kuperman, "Time machine in ocean acoustics," J. Acoust. Soc. Am. **153**(1), R1–R2 (2023).

[14] J. V. Candy, A. W. Meyer, A. J. Poggio, and B. L. Guidry, "Time-reversal processing for an acoustic communications experiment in a highly reverberant environment," J. Acoust. Soc. Am. **115**(4), 1621–1631 (2004).

[15] S. Yon, M. Tanter, and M. Fink, "Sound focusing in rooms: The time-reversal approach," J. Acoust. Soc. Am. **113**(3), 1533–1543 (2003).

[16] G. Ribay, J. de Rosny, and M. Fink, "Time reversal of noise sources in a reverberation room," J. Acoust. Soc. Am. **117**(5), 2866–2872 (2005).

[17] B. E. Anderson, T. J. Ulrich, P.-Y. Le Bas, and J. A. Ten Cate, "Three dimensional time reversal communications in elastic media," J. Acoust. Soc. Am. **139**(2), EL25–EL30 (2016).

[18] B. E. Anderson, "High amplitude time reversal focusing of sound and vibration," Proc. Mtgs. Acoust. **51**, 032001 (2023).

[19] J.-L. Thomas, F. Wu, and M. Fink, "Time reversal focusing applied to lithotripsy," Ultrason. Imag. **18**(2), 106–121 (1996).

[20] M. Tanter, J.-L. Thomas, and M. Fink, "Focusing and steering through absorbing and aberrating layers: Application to ultrasonic propagation through the skull," J. Acoust. Soc. Am. **103**(5), 2403–2410 (1998).

[21] G. Montaldo, P. Roux, A. Derode, C. Negreira, and M. Fink, "Ultrasound shock wave generator with one-bit time reversal in a dispersive medium, application to lithotripsy," Appl. Phys. Lett. **80**, 897–899 (2002).

[22] B. E. Anderson, M. Griffa, T. J. Ulrich, P.-Y. L. Bas, R. A. Guyer, and P. A. Johnson, "Crack localization and characterization in solid media using time reversal techniques," in *Proceedings of the 44th U.S. Rock Mechanics Symposium and 5th U.S.-Canada Rock Mechanics Symposium*, Salt Lake City, Utah (June 27–30, 2010), Paper No. 10–154.

[23] M. L. Willardson, B. E. Anderson, S. M. Young, M. H. Denison, and B. D. Patchett, "Time reversal focusing of high amplitude sound in a reverberation chamber," J. Acoust. Soc. Am. **143**(2), 696–705 (2018).

[24] C. B. Wallace and B. E. Anderson, "High-amplitude time reversal focusing of airborne ultrasound to generate a focused nonlinear difference frequency," J. Acoust. Soc. Am. **150**(2), 1411–1423 (2021).

[25] B. D. Patchett and B. E. Anderson, "Nonlinear characteristics of high amplitude focusing using time reversal in a reverberation chamber," J. Acoust. Soc. Am. **151**(6), 3603–3614 (2022).

[26] B. D. Patchett, B. E. Anderson, and A. D. Kingsley, "Numerical modeling of Mach-stem formation in high-amplitude time-reversal focusing," J. Acoust. Soc. Am. **153**(5), 2724–2732 (2023).

[27] C. Larmat, J.-P. Montagner, M. Fink, Y. Capdeville, A. Tourin, and E. Clevede, "Time-reversal imaging of seismic sources and applications to the great Sumatra earthquake," Geophys. Res. Lett. **33**(19), L19312, https://doi.org/10.1029/2006GL026336 (2006).

[28] C. Larmat, J. Tromp, Q. Liu, and J.-P. Montagner, "Time-reversal location of glacial earthquakes," J. Geophys. Res. **113**(B9), B09314, https://doi.org/10.1029/2008JB005607 (2008).

[29] C. Larmat, R. A. Guyer, and P. A. Johnson, "Tremor source location using time-reversal: Selecting the appropriate imaging field," Geophys. Res. Lett. **36**(22), L22304, https://doi.org/10.1029/2009GL040099 (2009).

[30] C. S. Larmat, R. A. Guyer, and P. A. Johnson, "Time-reversal methods in geophysics," Phys. Today **63**(8), 31–35 (2010).

[31] R. K. Ing and N. Quieffin, "In solid localization of finger impacts using acoustic time-reversal process," Appl. Phys. Lett **87**(20), 204104 (2005).

[32] D. Vigoureux and J.-L. Guyader, "A simplified time reversal method used to localize vibrations sources in a complex structure," Appl. Acoust. **73**(5), 491–496 (2012).

[33] D. G. Albert, L. Liu, and M. L. Moran, "Time reversal processing for source location in an urban environment (L)," J. Acoust. Soc. Am. **118**(2), 616–619 (2005).

[34] S. Cheinet, L. Ehrhardt, and T. Broglin, "Impulse source localization in an urban environment: Time reversal versus time matching," J. Acoust. Soc. Am. **139**(1), 128–140 (2016).

[35] C. Heaton, B. E. Anderson, and S. M. Young, "Time reversal focusing of elastic waves in plates for educational demonstration purposes," J. Acoust. Soc. Am. **141**(2), 1084–1092 (2017).

[36] L. A. Barnes, B. E. Anderson, P.-Y. Le Bas, A. D. Kingsley, A. C. Brown, and H. R. Thomsen, "The physics of knocking over LEGO mini-figures with time reversal focused vibrations," J. Acoust. Soc. Am. **151**(2), 738–751 (2022).

[37] A. A. Maznev and O. B. Wright, "Upholding the diffraction limit in the focusing of light and sound," Wave Motion **68**, 182–189 (2017).

[38] E. D. Golightly, B. E. Anderson, A. D. Kingsley, R. Russell, and R. Higgins, "Super resolution, time reversal focusing using path diverting properties of scatterers," Appl. Acoust. **206**, 109308 (2023).

[39] A. D. Kingsley, B. E. Anderson, and T. J. Ulrich, "Super-resolution within a one-dimensional phononic crystal of resonators using time reversal in an equivalent circuit model," J. Acoust. Soc. Am. **152**(3), 1263–1271 (2022).

[40] G. Lerosey, J. de Rosny, A. Tourin, and M. Fink, "Focusing beyond the diffraction limit with far-field time reversal," Science **315**(5815), 1120–1122 (2007).

[41] F. Lemoult, M. Fink, and G. Lerosey, "Acoustic resonators for far-field control of sound on a subwavelength scale," Phys. Rev. Lett. **107**(6), 064301 (2011).

[42] F. Lemoult, N. Kaina, M. Fink, and G. Lerosey, "Soda cans metamaterial: A subwavelength-scaled phononic crystal," Crystals **6**(7), 82 (2016).

[43] A. A. Maznev, G. Gu, S. Y. Sun, J. Xu, Y. Shen, N. Fang, and S. Y. Zhang, "Extraordinary focusing of sound above a soda can array without time reversal," New J. Phys. **17**(4), 042001 (2015).

[44] A. D. Kingsley and B. E. Anderson, "Time reversal in a phononic crystal using finite-element modeling and an equivalent circuit model," JASA Express Lett. **2**(12), 124002 (2022).

[45] A. D. Kingsley, A. Basham, and B. E. Anderson, "Time reversal imaging of complex sources in a three-dimensional environment using a spatial inverse filter," J. Acoust. Soc. Am. **154**(2), 1018–1027 (2023).

[46] F. Lemoult, N. Kaina, M. Fink, and G. Lerosey, "Wave propagation control at the depp subwavelength scale in metamaterials," Nat. Phys. **9**, 55–60 (2013).

[47] A. S. Gliozzi, M. Miniaci, F. Bosia, N. M. Pugno, and M. Scalerandi, "Metamaterials-based sensor to detect and locate nonlinear elastic sources," Appl. Phys. Lett. **107**, 161902 (2015).

[48] M. Miniaci, A. S. Gliozzi, B. Morvan, A. Krushynska, F. Bosia, M. Scalerandi, and N. M. Pugno, "Proof of concept for an ultrasensitive technique to detect and localize sources of elastic nonlinearity using phononic crystals," Phys. Rev. Lett. **118**, 214301 (2017).

[49] A. D. Kingsley, J. M. Clift, B. E. Anderson, J. E. Ellsworth, T. J. Ulrich, and P.-Y. L. Bas, "Development of software for performing acoustic time reversal with multiple inputs and outputs," Proc. Mtgs. Acoust. **46**, 055003 (2022).

[50] B. D. Patchett, B. E. Anderson, and A. D. Kingsley, "The impact of room location on time reversal focusing amplitudes," J. Acoust. Soc. Am. **150**(2), 1424–1433 (2021).

[51]ISO 3741:2010, "Sound power and energy in reverberant environments" (International Organization for Standardization, Geneva, Switzerland, 2010).

[52]S. M. Young, B. E. Anderson, R. C. Davis, R. R. Vanfleet, and N. B. Morrill, "Sound transmission measurements through porous screen," Proc. Mtgs. Acoust. **26**, 045003 (2017).

[53]F. J. Fahy, *Sound Intensity*, 2nd ed. (Routledge and CRC Press, London, UK, 2017), p. 95.

[54]J. S. Lawrence, K. L. Gee, T. B. Neilsen, and S. D. Sommerfeldt, "Highly directional pressure sensing using the phase gradient," J. Acoust. Soc. Am. **144**(4), EL346–EL352 (2018).